Footprint of New Physics in $b \to c\tau\bar{\nu}$ Transition

Ying Li

Yantai University （烟台大学）

In collaboration with ZR Huang, CD Lu

The 3rd IBS-KIAS Joint Workshop,2019

Outline

- Background and Motivation
- The status of R(D),R(D*) and R(J/psi)
- Hadronic Form Factors

  B—>D&D*

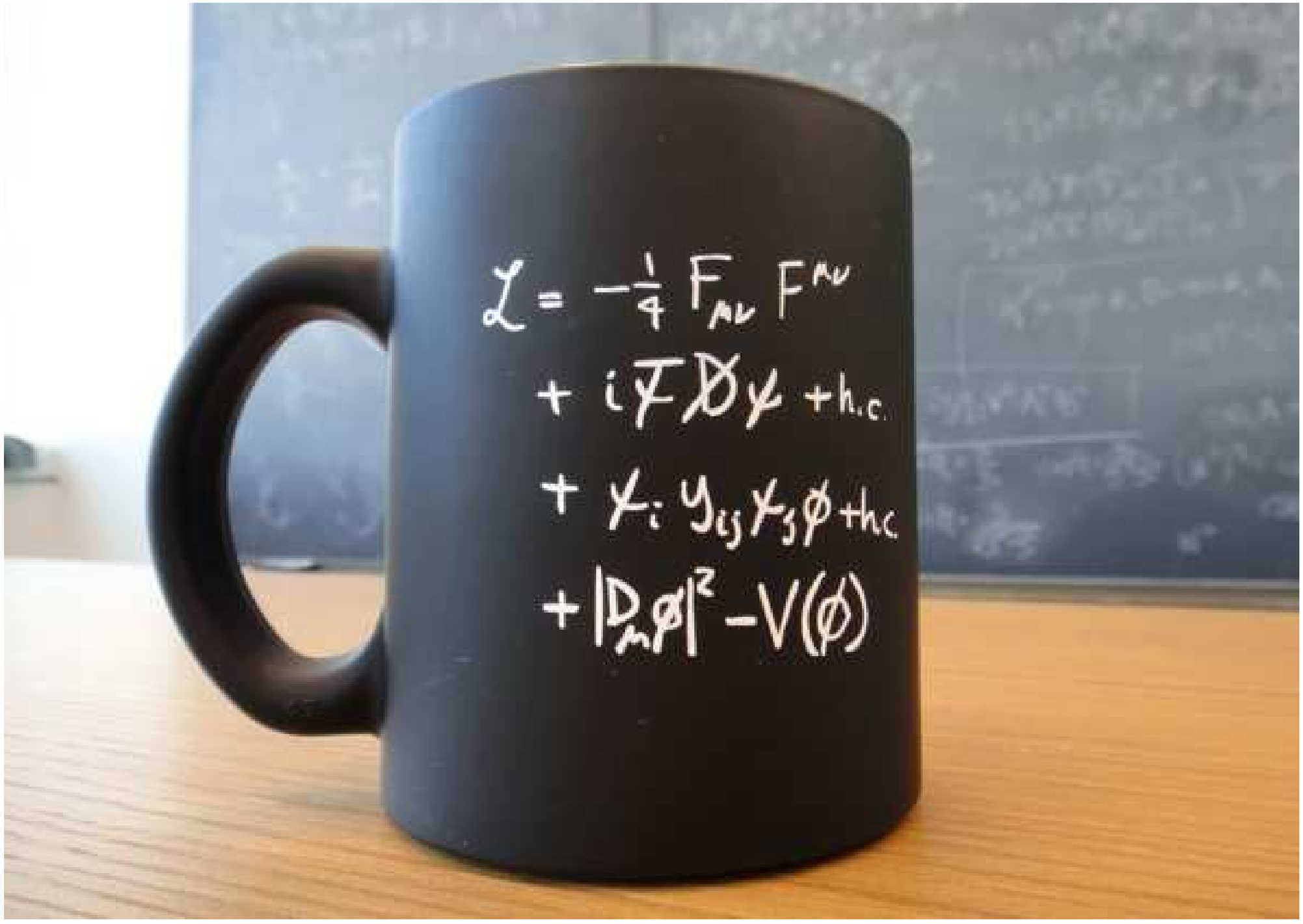
  Bc—>J/psi
- Numerical Results

  Method

  Constraints on Wilson Coefficients

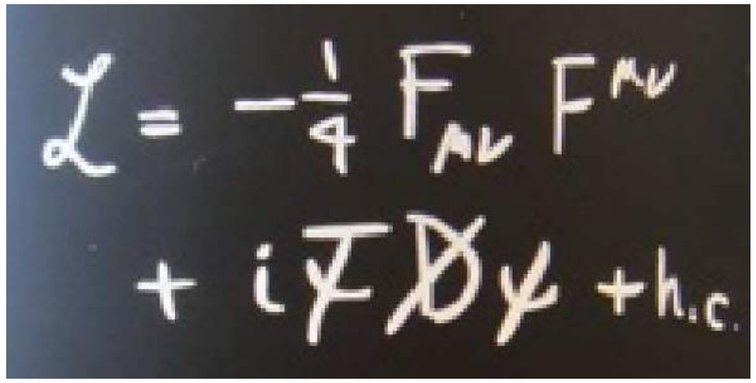
  Predictions
- Summary

The Standard Model of Particle Physics



Flavor and Proliferation of Parameters

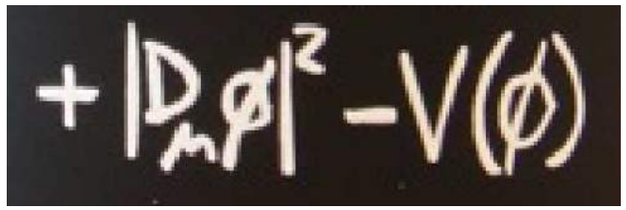
gauge sector



describes the gauge interactions of the quarks and leptons

parametrized by
3 gauge couplings
g_1, g_2, g_3

Higgs sector



breaks electro-weak symmetry and gives mass to the $W^\pm$ and Z bosons

2 free parameters
Higgs mass
Higgs vev

flavor sector



leads to masses and mixings of the quarks and leptons

22 free parameters
to describe the masses and mixings of the quarks and leptons

The most unknown sector in SM!

Spectacular Track Record

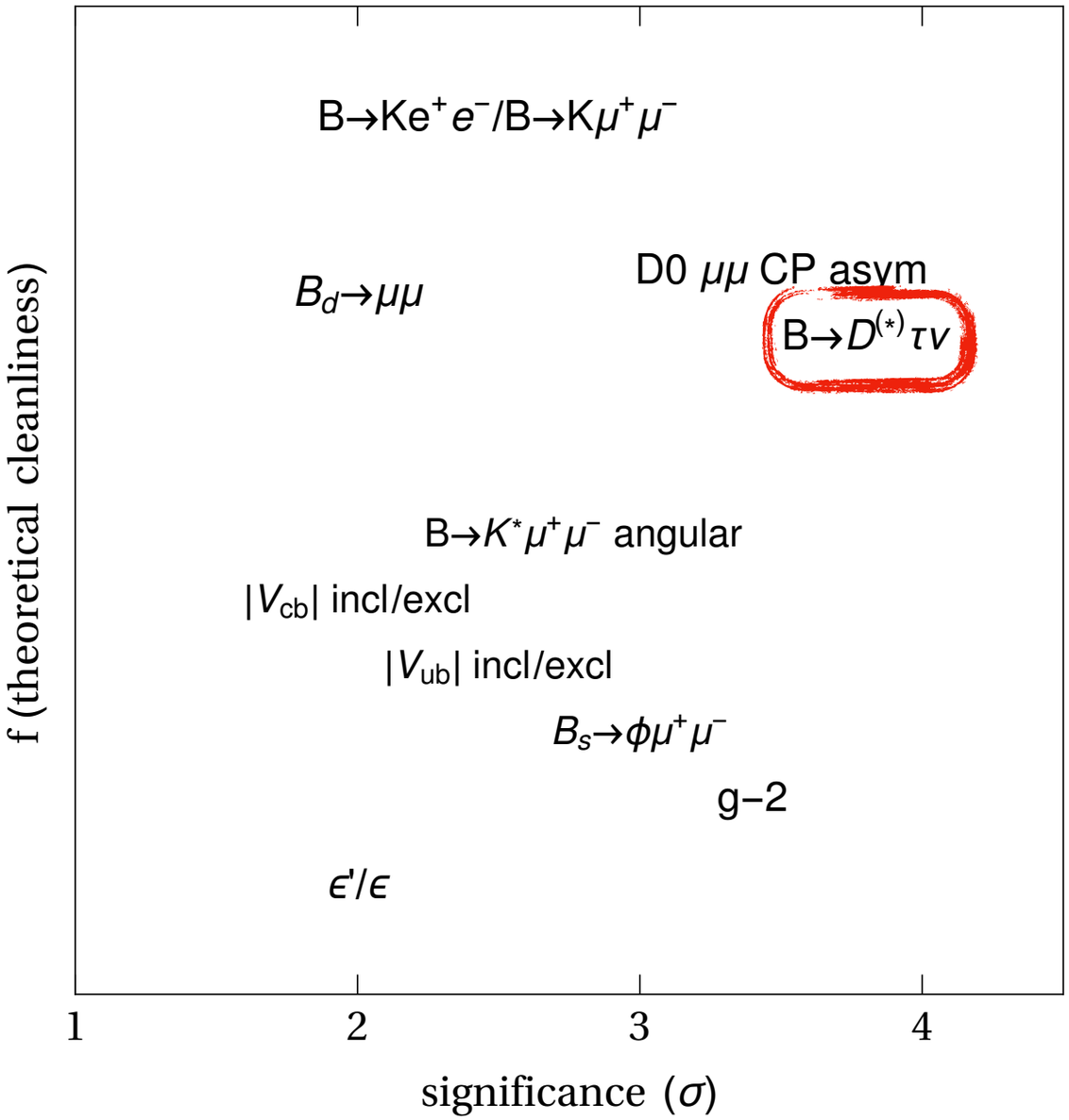
See Cai-Dian's talk

- Searching for new physics via virtual effects has been extremely successful
- Flavor physics was crucial to figure out $\mathcal{L}_{\rm SM}$:
  - Absence of $K_L \to \mu\mu$ predicted charm (Glashow, Iliopoulos, Maiani)
  - ϵ_K predicted 3rd generation (Kobayashi & Maskawa)
  - Δm_K predicted m_c (Gaillard & Lee; Vainshtein & Khriplovich)
  - Δm_B predicted large m_t
- Likely to be important to figure out $\mathcal{L}_{\rm BSM}$ as well
- If new physics discovered, want to probe it in as many different ways as possible

Now, we may have some hints of new physics in FLAVOUR PHYSICS.

Status of Flavor Anomalies

See Lu and Ro's talk



✔ Some would be unambiguous NP signals

✔Except for theoretically cleanest modes, cross-checks needed to build robust case

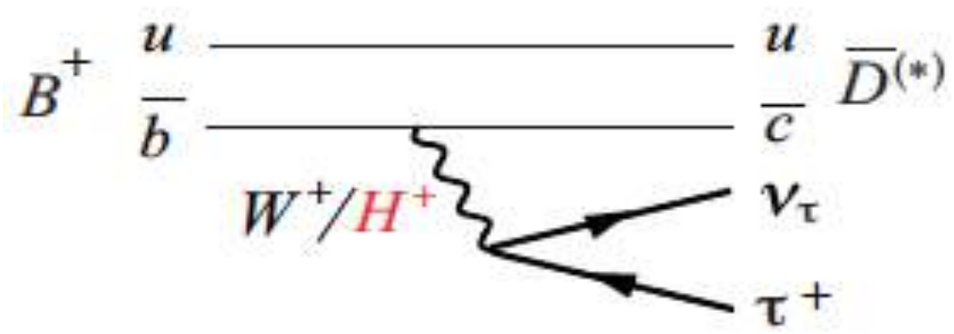
– measurements of related observables

– independent theory / lattice calc.

✔ Few of these are where NP was expected to show up, even just 5–10 years ago

✔ Each could be an hour talk...

The B → D(*)τ ν⁻ Anomaly



Br~0.7+1.3% in SM.
Not rare, but with two missing neutrinos.

$$R(D^{(*)}) := \frac{\mathcal{B}(\bar{B} \to D^{(*)}\tau\bar{\nu}_\tau)}{\mathcal{B}(\bar{B} \to D^{(*)}\ell\bar{\nu}_\ell)}$$

Z. Phys, C46, 93 (1990)

- S.L. decays involving a $\tau^{\pm}$ have an additional helicity amplitude (for D*τν)

$$\frac{d\Gamma}{dq^2} = \frac{G_F^2 |V_{cb}|^2 \left|\mathbf{p}^*_{D^{(*)}}\right| q^2}{96\pi^3 m_B^2} \left(1 - \frac{m_\tau^2}{q^2}\right)^2 \left[\left(|H_+|^2 + |H_-|^2 + |H_0|^2\right)\left(1 + \frac{m_\tau^2}{2q^2}\right) + \frac{3m_\tau^2}{2q^2}|H_s|^2\right]$$

For Dτν, H_+ and H_- do not contribute!

- A charged Higgs (2HDM type II) of spin 0 coupling to the τ will only affect H_s

$$H_s^{2HDM} = H_s^{SM} \times \left(1 - \frac{\tan^2\beta}{m_H^2} \frac{q^2}{1 \mp \frac{m_c}{m_b}}\right)$$

\- for Dτν
\+ for D*τν

PRD 78, 015006 (2008)
PhD 85, 094025 (2012)

This could enhance or decrease the BF, depending on $\tan\beta/m_H$

The B → D(*)τ ν⁻ Anomaly

A charged Higgs(2HDM type II)of spin0 coupling to the τ will only affect H_S

$$H_s^{2HDM} = H_s^{SM} \times \left(1 - \frac{\tan^2\beta}{m_H^2} \frac{q^2}{1 \mp \frac{m_c}{m_b}}\right)$$

We estimate the effect of 2HDM, accounting for difference in signal yield and efficiency.

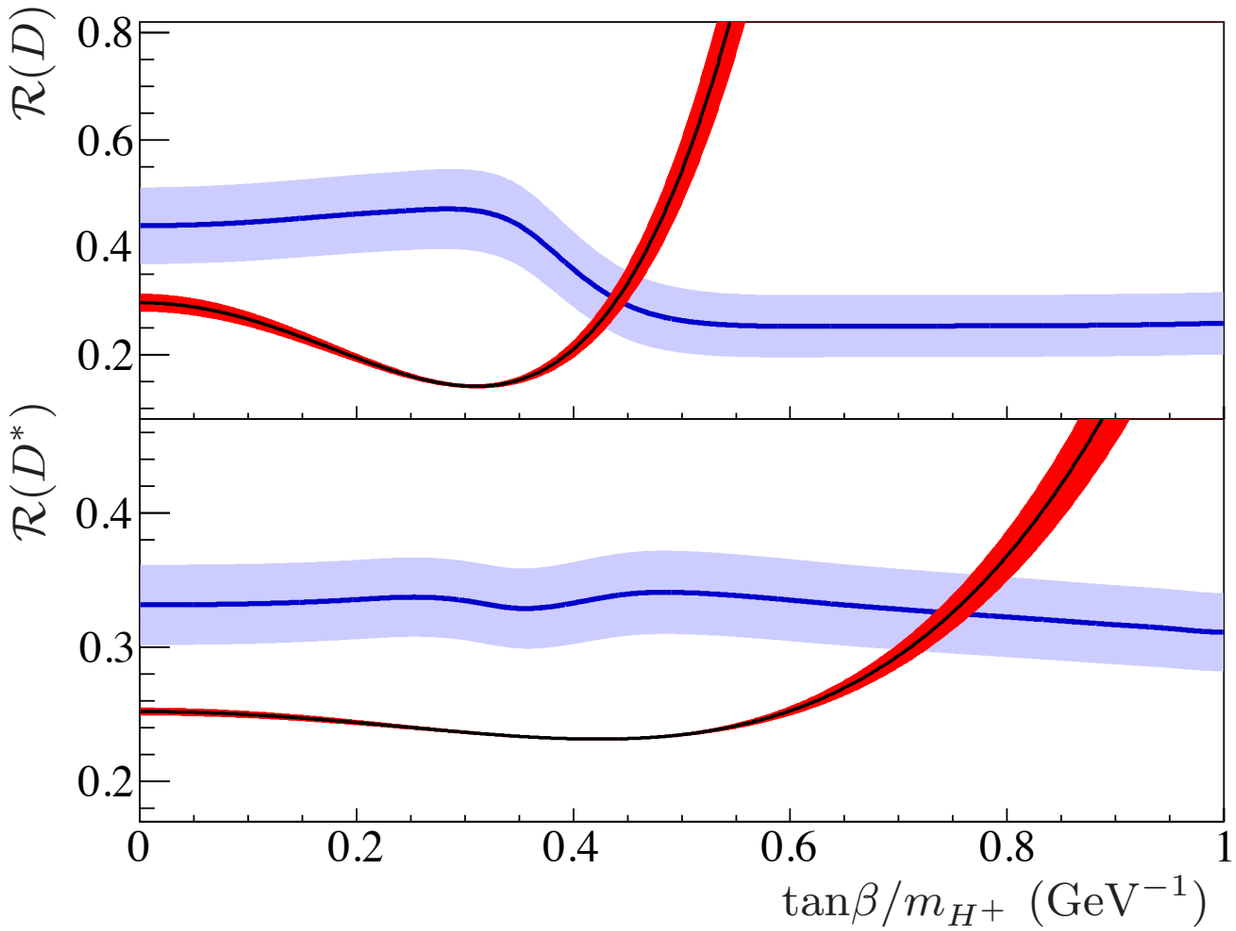
The data match 2HDM Type II contribution at

$\tan\beta/m_H = 0.44 \pm 0.02$ for R(D)

$\tan\beta/m_H = 0.75 \pm 0.04$ for R(D*)

The combination of R(D) and R(D*)

excludes the Type II 2HDM in the full $\tan\beta$-m_H parameter space with P >99.8%, provided M_H>15 GeV !



arXiv: 1205.5442, PRL.109.101802(2012)

Lepton Flavour Universal

Ratio of branching fractions

$$R(D^{(*)}) := \frac{\mathcal{B}(\bar{B} \to D^{(*)}\tau\bar{\nu}_\tau)}{\mathcal{B}(\bar{B} \to D^{(*)}\ell\bar{\nu}_\ell)} \qquad \ell = e, \mu$$

Predictable in the SM: Source of LFNU = mass

Smaller theoretical errors in the SM (and beyond)

No Vcb in the ratio

Form factor uncertainty tends to cancel.

Controlled by

$\bar{B} \to D^{(*)}\ell\bar{\nu}_\ell$ experimental data, lattice QCD,

Heavy Quark Effective Theory, QCD sum rule

SM Predictions

$R(D) = 0.302 \pm 0.015$ (Tanaka, Wantanabe, 2010,HQET)

0.296 ± 0.016 (Fajfer, Kamenik, Nisandzic, 2012, HQET)

0.299 ± 0.011 (Bailey et al., 2015, lattice)

0.300 ± 0.008 (Na et al., 2015, lattice)

0.299 ± 0.003 (Bigi, Gambino, 2016, combined)

0.299 ± 0.003 (Bernlochner et al., 2017, combined)

$0.407 \pm 0.039 \pm 0.024$ (Exp. HFLAV, 2017) $2.3\ \sigma$

$R(D^*) = 0.252 \pm 0.003$ (Fajfer, Kamenik, Nisandzic, 2012, HQET)

0.252 ± 0.004 (Tanaka, Wantanabe, 2013,HQET)

0.257 ± 0.003 (Bernlochner et al., 2017, combined)

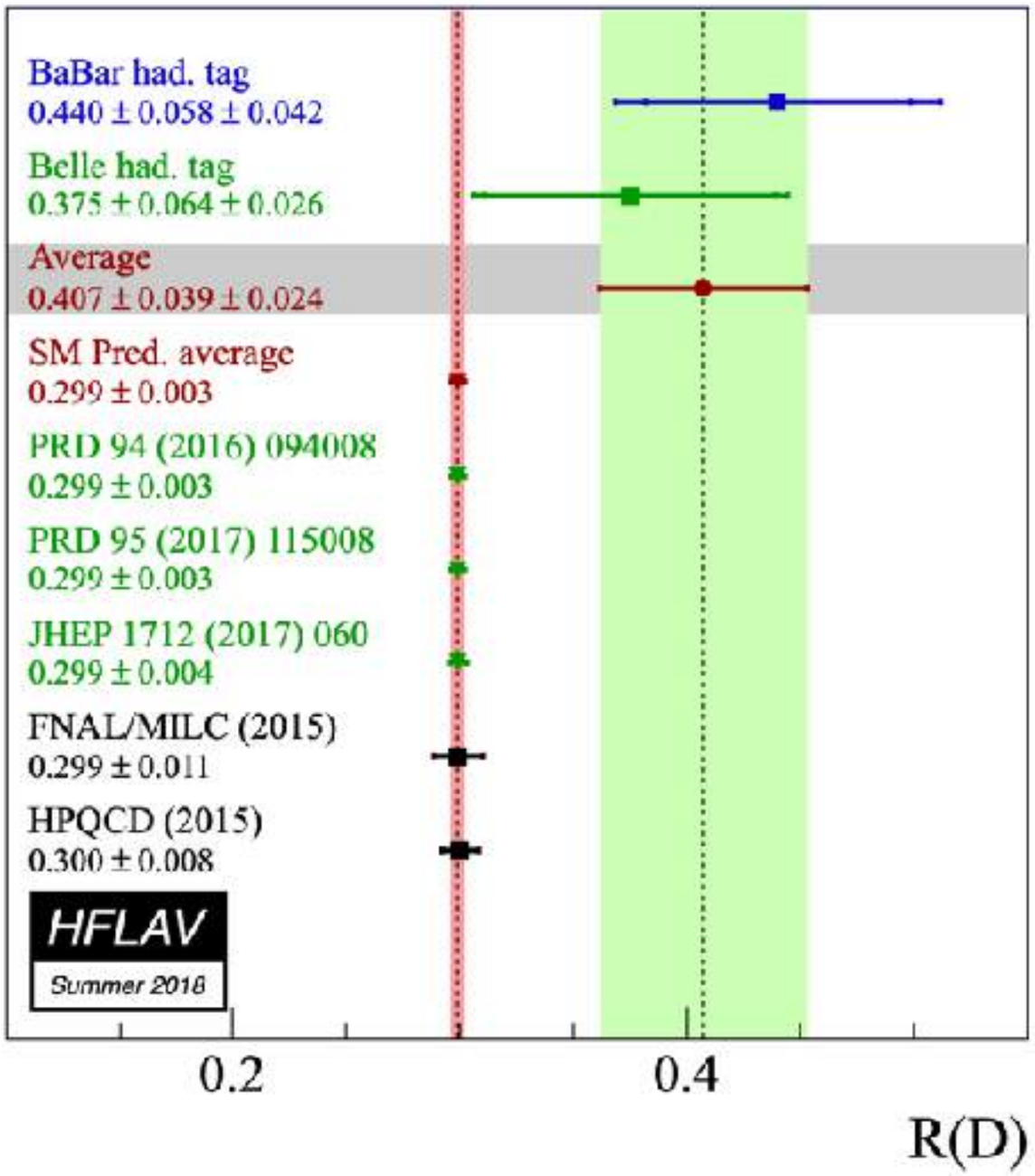
0.260 ± 0.008 (Bigi, Gambino, Schacht, 2017, combined)

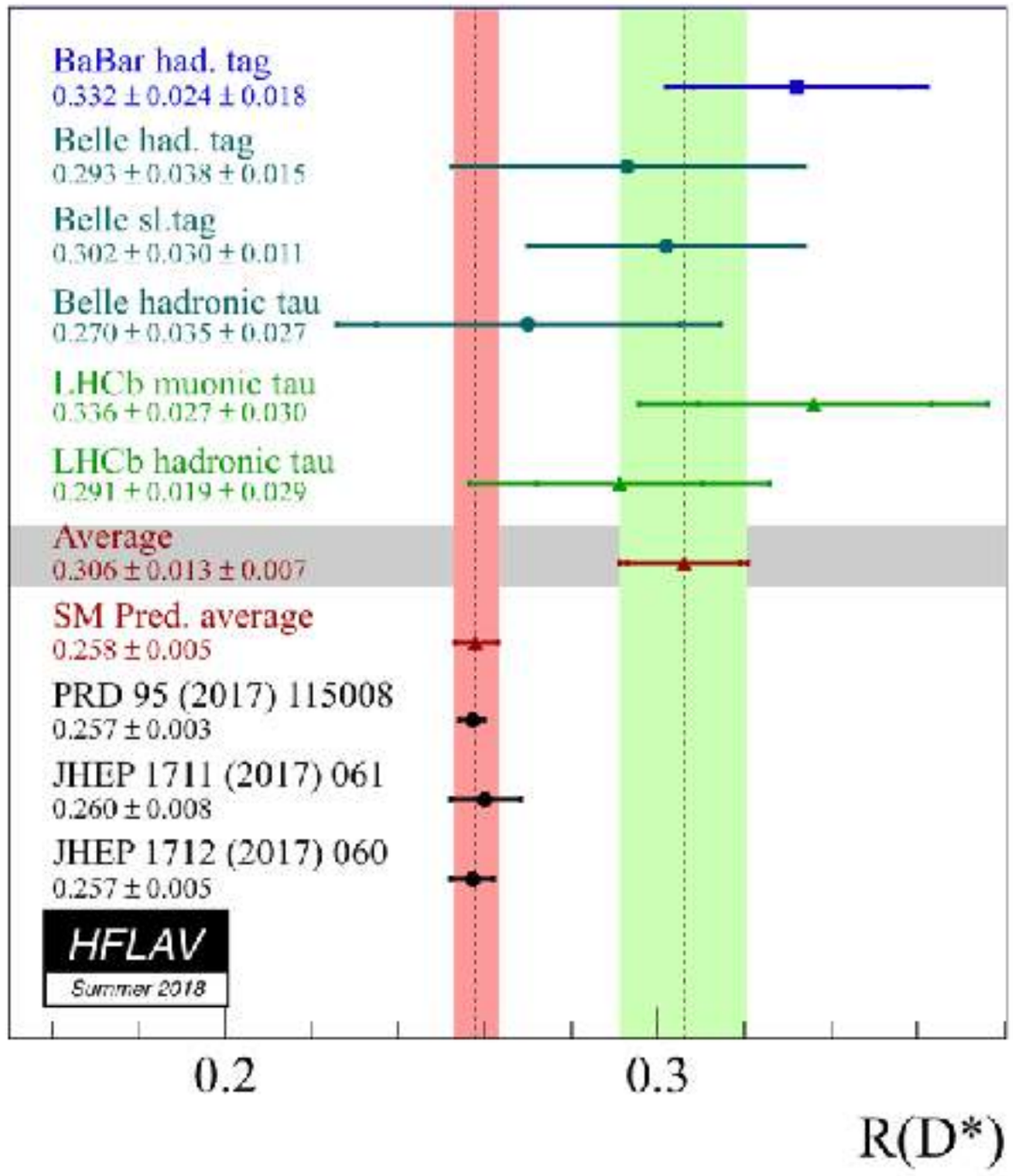
0.259 ± 0.006 (Jaiswal, Nandi, Patra, 2017, CLN)

0.257 ± 0.005 (Jaiswal, Nandi, Patra, 2017, BGL)

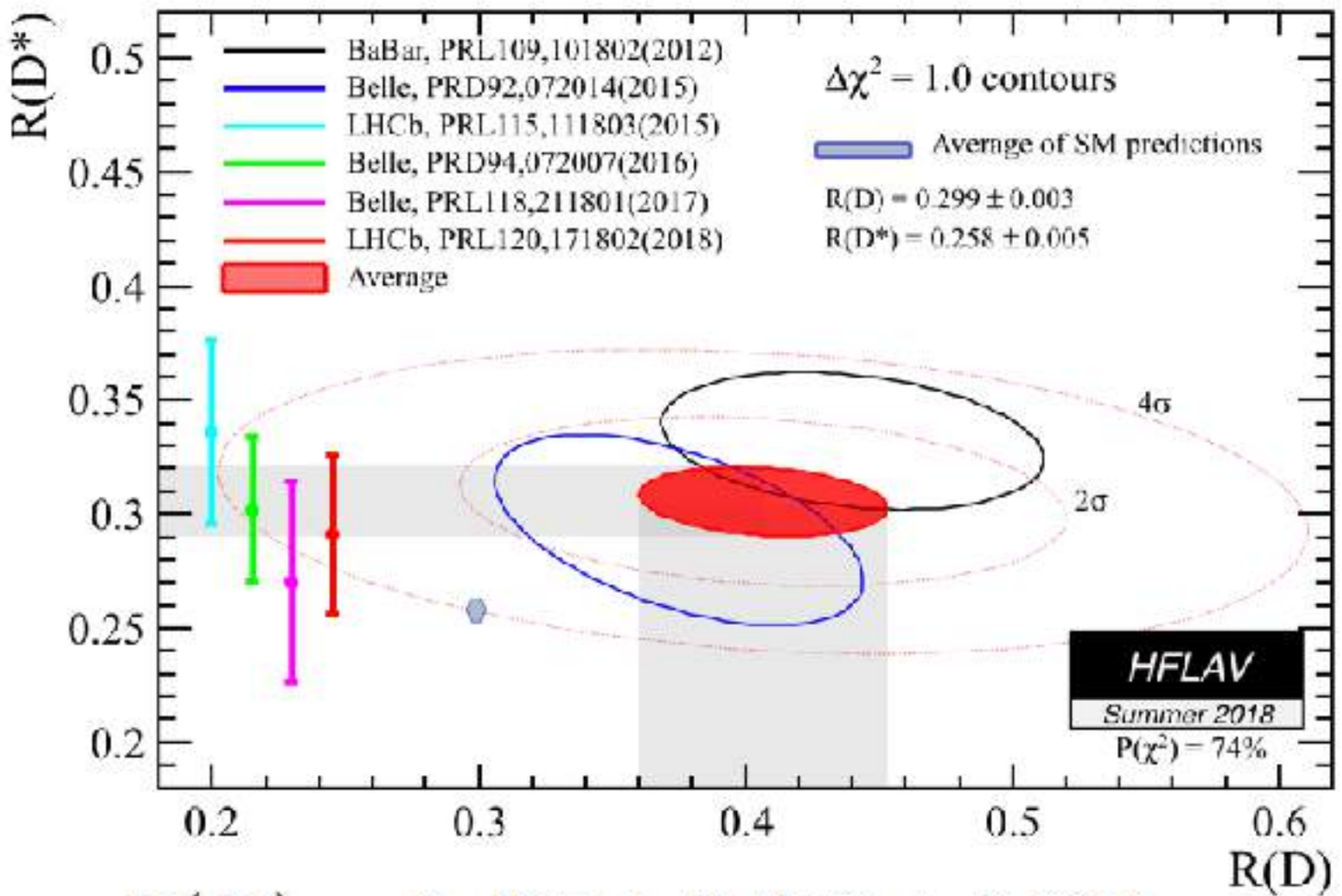
$0.304 \pm 0.013 \pm 0.007$ (Exp. HFLAV, 2017) $3.4\ \sigma$

Experiments and status of SM





Experiments and status of SM



$$R(D) = 0.407 \pm 0.039 \pm 0.024$$

$$R(D^*) = 0.304 \pm 0.013 \pm 0.007$$

$\sim$3.6 σ **2018**

$B_c \to J/\psi l\nu$

The same quark-level process

$$R(J/\psi) := \frac{\mathcal{B}(B_c \to J/\psi\, \tau\bar{\nu}_\tau)}{\mathcal{B}(B_c \to J/\psi\, \ell\bar{\nu}_\ell)}$$

Experiment: $R(J/\psi) = 0.71 \pm 0.17 \pm 0.18$ LHCb

PRL120, 121801 (2018)

SM prediction

Form factors similar to $\bar{B} \to D^*$, but less accurate

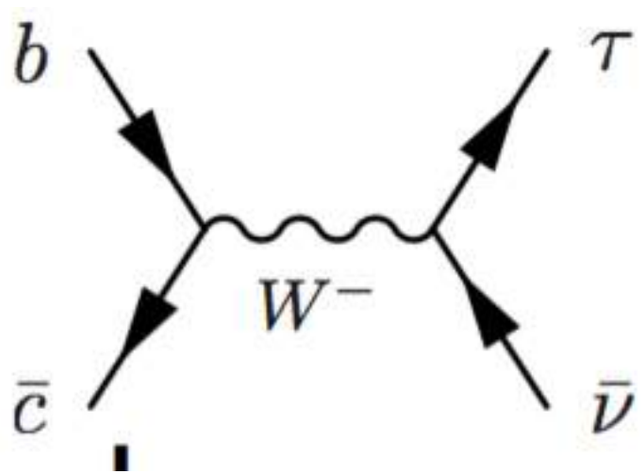
$R(J/\psi)_{\rm SM} = [0.279,\ 0.301]$ R. Dutta, A. Bhol PRD96, 076001 (2017)

$= 0.283 \pm 0.048$ R. Watanabe, PLB776 (2018) 5

~1.7 σ

W.F. Wang, Y.Y. Fan, Z.J. Xiao, Chin. Phys. C 37 (2013) 093102

Bc—>Tau v



$$\mathrm{Br}(B_c \to \tau\bar{\nu}) = \tau_{B_c} \frac{1}{8\pi} m_{B_c} m_\tau^2 \left(1 - \frac{m_\tau^2}{m_{B_c}^2}\right)^2 f_{B_c}^2 G_F^2 |V_{cb}|^2$$

$$\times \left| 1 + C_{V_1} - C_{V_2} + \frac{m_{B_c}^2}{m_\tau (m_b + m_c)} (C_{S_1} - C_{S_2}) \right|^2$$

Consider redundant set of operators

SM

	Operator		Fierz identity	Allowed Current	$\delta\mathcal{L}_{\text{int}}$
$\mathcal{O}_{V_L}$	$(\bar{c}\gamma_\mu P_L b)\,(\bar{\tau}\gamma^\mu P_L \nu)$			$(1,3)_0$	$(g_q \bar{q}_L \boldsymbol{\tau}\gamma^\mu q_L + g_\ell \bar{\ell}_L \boldsymbol{\tau}\gamma^\mu \ell_L) W'_\mu$
$\mathcal{O}_{V_R}$	$(\bar{c}\gamma_\mu P_R b)\,(\bar{\tau}\gamma^\mu P_L \nu)$				
$\mathcal{O}_{S_R}$	$(\bar{c}P_R b)\,(\bar{\tau}P_L \nu)$			$\Big\rangle (1,2)_{1/2}$	$(\lambda_d \bar{q}_L d_R \phi + \lambda_u \bar{q}_L u_R i\tau_2 \phi^\dagger + \lambda_\ell \bar{\ell}_L e_R \phi)$
$\mathcal{O}_{S_L}$	$(\bar{c}P_L b)\,(\bar{\tau}P_L \nu)$				
$\mathcal{O}_T$	$(\bar{c}\sigma^{\mu\nu}P_L b)\,(\bar{\tau}\sigma_{\mu\nu}P_L \nu)$				
$\mathcal{O}'_{V_L}$	$(\bar{\tau}\gamma_\mu P_L b)\,(\bar{c}\gamma^\mu P_L \nu)$	$\longleftrightarrow$	$\mathcal{O}_{V_L}\Big\langle$	$(3,3)_{2/3}$	$\lambda\, \bar{q}_L \boldsymbol{\tau}\gamma_\mu \ell_L \boldsymbol{U}^\mu$
$\mathcal{O}'_{V_R}$	$(\bar{\tau}\gamma_\mu P_R b)\,(\bar{c}\gamma^\mu P_L \nu)$	$\longleftrightarrow$	$-2\mathcal{O}_{S_R}$	$\Big\rangle (3,1)_{2/3}$	$(\lambda\, \bar{q}_L \gamma_\mu \ell_L + \tilde{\lambda}\, \bar{d}_R \gamma_\mu e_R) U^\mu$
$\mathcal{O}'_{S_R}$	$(\bar{\tau}P_R b)\,(\bar{c}P_L \nu)$	$\longleftrightarrow$	$-\frac{1}{2}\mathcal{O}_{V_R}$		
$\mathcal{O}'_{S_L}$	$(\bar{\tau}P_L b)\,(\bar{c}P_L \nu)$	$\longleftrightarrow$	$-\frac{1}{2}\mathcal{O}_{S_L} - \frac{1}{8}\mathcal{O}_T$	$(3,2)_{7/6}$	$(\lambda\, \bar{u}_R \ell_L + \tilde{\lambda}\, \bar{q}_L i\tau_2 e_R) R$
$\mathcal{O}'_T$	$(\bar{\tau}\sigma^{\mu\nu}P_L b)\,(\bar{c}\sigma_{\mu\nu}P_L \nu)$	$\longleftrightarrow$	$-6\mathcal{O}_{S_L} + \frac{1}{2}\mathcal{O}_T$		
$\mathcal{O}''_{V_L}$	$(\bar{\tau}\gamma_\mu P_L c^c)\,(\bar{b}^c\gamma^\mu P_L \nu)$	$\longleftrightarrow$	$-\mathcal{O}_{V_R}$		
$\mathcal{O}''_{V_R}$	$(\bar{\tau}\gamma_\mu P_R c^c)\,(\bar{b}^c\gamma^\mu P_L \nu)$	$\longleftrightarrow$	$-2\mathcal{O}_{S_R}$	$(\bar{3},2)_{5/3}$	$(\lambda\, \bar{d}^c_R \gamma_\mu \ell_L + \tilde{\lambda}\, \bar{q}^c_L \gamma_\mu e_R) V^\mu$
$\mathcal{O}''_{S_R}$	$(\bar{\tau}P_R c^c)\,(\bar{b}^c P_L \nu)$	$\longleftrightarrow$	$\frac{1}{2}\mathcal{O}_{V_L}\Big\langle$	$(\bar{3},3)_{1/3}$	$\lambda\, \bar{q}^c_L i\tau_2 \boldsymbol{\tau} \ell_L \boldsymbol{S}$
$\mathcal{O}''_{S_L}$	$(\bar{\tau}P_L c^c)\,(\bar{b}^c P_L \nu)$	$\longleftrightarrow$	$-\frac{1}{2}\mathcal{O}_{S_L} + \frac{1}{8}\mathcal{O}_T$	$\Big\rangle (\bar{3},1)_{1/3}$	$(\lambda\, \bar{q}^c_L i\tau_2 \ell_L + \tilde{\lambda}\, \bar{u}^c_R e_R) S$
$\mathcal{O}''_T$	$(\bar{\tau}\sigma^{\mu\nu}P_L c^c)\,(\bar{b}^c\sigma_{\mu\nu}P_L \nu)$	$\longleftrightarrow$	$-6\mathcal{O}_{S_L} - \frac{1}{2}\mathcal{O}_T$		

Model-independent approach

Effective Lagrangian for $b \to c\tau\bar{\nu}$

all possible 4f operators with LH neutrinos

$$-\mathcal{L}_{\text{eff}} = 2\sqrt{2}G_F V_{cb} \sum_{l=e,\mu,\tau} \left[(\delta_{l\tau} + C_{V_1}^l)\mathcal{O}_{V_1}^l + C_{V_2}^l \mathcal{O}_{V_2}^l + C_{S_1}^l \mathcal{O}_{S_1}^l + C_{S_2}^l \mathcal{O}_{S_2}^l + C_T^l \mathcal{O}_T^l\right]$$

SM

$$\begin{aligned}
\mathcal{O}_{V_1}^l &= \bar{c}_L \gamma^\mu b_L \, \bar{\tau}_L \gamma_\mu \nu_{Ll} \,, && \text{SM-like, RPV, LQ,W'} \\
\mathcal{O}_{V_2}^l &= \bar{c}_R \gamma^\mu b_R \, \bar{\tau}_L \gamma_\mu \nu_{Ll} \,, && \text{RH current} \\
\mathcal{O}_{S_1}^l &= \bar{c}_L b_R \, \bar{\tau}_R \nu_{Ll} \,, && \text{charged Higgs II, RPV, LQ} \\
\mathcal{O}_{S_2}^l &= \bar{c}_R b_L \, \bar{\tau}_R \nu_{Ll} \,, && \text{charged Higgs III, LQ} \\
\mathcal{O}_T^l &= \bar{c}_R \sigma^{\mu\nu} b_L \, \bar{\tau}_R \sigma_{\mu\nu} \nu_{Ll} && \text{LQ}
\end{aligned}$$

Form Factor

HQET

$$
\begin{aligned}
\langle D(k)|\bar{c}\gamma^{\mu}b|\overline{B}(p)\rangle &= \sqrt{m_B m_D}\left[h_+(w)(v+v')^{\mu}+h_-(w)(v-v')^{\mu}\right], \\
\langle D(k)|\bar{c}b|\bar{B}(p)\rangle &= \sqrt{m_B m_D}(w+1)h_S(w), \\
\langle D(k)|\bar{c}\sigma^{\mu\nu}b|\bar{B}(p)\rangle &= -i\sqrt{m_B m_D}h_T(w)(v^{\mu}v'^{\nu}-v^{\nu}v'^{\mu}), \\
\langle D^*(k,\epsilon)|\bar{c}\gamma^{\mu}b|\bar{B}(p)\rangle &= i\sqrt{m_B m_{D^*}}\,h_V(w)\varepsilon^{\mu\nu\rho\sigma}\epsilon^*_{\nu}v'_{\rho}v_{\sigma}, \\
\langle D^*(k,\epsilon)|\bar{c}\gamma^{\mu}\gamma^5 b|\bar{B}(p)\rangle &= \sqrt{m_B m_{D^*}}\left[h_{A_1}(w)(w+1)\epsilon^{*\mu}\right. \\
&\quad \left.-(\epsilon^*\cdot v)\left(h_{A_2}(w)v^{\mu}+h_{A_3}(w)v'^{\mu}\right)\right], \\
\langle D^*(k,\epsilon)|\bar{c}\gamma^5 b|\bar{B}(p)\rangle &= -\sqrt{m_B m_{D^*}}\,(\epsilon^*\cdot v)h_P(w), \\
\langle D^*(k,\epsilon)|\bar{c}\sigma^{\mu\nu}b|\bar{B}(p)\rangle &= -\sqrt{m_B m_{D^*}}\,\varepsilon^{\mu\nu\rho\sigma}\Big[h_{T_1}(w)\epsilon^*_{\rho}(v+v')_{\sigma}+h_{T_2}(w)\epsilon^*_{\rho}(v-v')_{\sigma} \\
&\quad +h_{T_3}(w)(\epsilon^*\cdot v)v_{\rho}v'_{\sigma}\Big],
\end{aligned}
$$

F. U. Bernlochner, Z. Ligeti, M. Papucci, and D. J. Robinson, Phys. Rev. D95, 115008 (2017)

Form Factor

In the heavy quark limit, only the single leading Isgur-Wise function $\xi(w)$ is needed for expressing the $B \to D^{(*)}$ form factors. With inclusion of the $\mathcal{O}(\alpha_s, \Lambda_{\rm QCD}/m_{b,c})$ contributions, these form factors are written as

$$h_+ = \xi\left\{1 + \hat{\alpha}_s\left[C_{V_1} + \frac{w+1}{2}\,(C_{V_2} + C_{V_3})\right] + (\varepsilon_c + \varepsilon_b)\,\hat{L}_1\right\},$$

$$h_- = \xi\left[\hat{\alpha}_s\,\frac{w+1}{2}\,(C_{V_2} - C_{V_3}) + (\varepsilon_c - \varepsilon_b)\,\hat{L}_4\right],$$

$$h_S = \xi\left[1 + \hat{\alpha}_s\,C_S + (\varepsilon_c + \varepsilon_b)\left(\hat{L}_1 - \hat{L}_4\,\frac{w-1}{w+1}\right)\right],$$

$$h_T = \xi\left[1 + \hat{\alpha}_s(C_{T_1} - C_{T_2} + C_{T_3}) + (\varepsilon_c + \varepsilon_b)(\hat{L}_1 - \hat{L}_4)\right],$$

Form Factor

The $L_{1\ldots6}$ functions can be expressed in terms of the sub-leading Isgur-Wise functions through:

$$\hat{L}_1 = -4(w-1)\hat{\chi}_2 + 12\hat{\chi}_3\,, \qquad \hat{L}_2 = -4\hat{\chi}_3\,, \qquad \hat{L}_3 = 4\hat{\chi}_2\,,$$
$$\hat{L}_4 = 2\eta - 1\,, \qquad \hat{L}_5 = -1\,, \qquad \hat{L}_6 = -2(1+\eta)/(w+1)\,.$$

With $\hat{\chi}_3(1) = 0$ implied by the Luke's theorem, up to $\mathcal{O}(\varepsilon_{c,b}(w-1))$ the subleading Isgur-Wise functions can be approximated as follows:

$$\hat{\chi}_2(w) \simeq \hat{\chi}_2(1) + \hat{\chi}_2'(1)(w-1)\,, \quad \hat{\chi}_3(w) \simeq \hat{\chi}_3'(1)(w-1)\,,$$
$$\eta(w) \simeq \eta(1) + \eta'(1)(w-1)\,.$$

Form Factor

- Lattice QCD at zero hadronic recoil
- Light-cone sum rule at large hadronic recoil
- Strong unitarity constraints
- 1S Scheme (ensuring the renormalon cancellation)

$$\begin{pmatrix} \chi_2(1) \\ \chi_2'(1) \\ \chi_3'(1) \\ \eta(1) \\ \eta'(1) \\ \rho^2 \\ c \\ \delta_{h_{A_1}} \\ \delta_{h_+} \end{pmatrix} = \begin{pmatrix} -0.058 \pm 0.019 \\ -0.001 \pm 0.020 \\ 0.035 \pm 0.019 \\ 0.358 \pm 0.043 \\ 0.044 \pm 0.125 \\ 1.306 \pm 0.059 \\ 1.220 \pm 0.109 \\ -2.299 \pm 0.394 \\ 0.485 \pm 0.269 \end{pmatrix},$$

M. Jung and D. M. Straub, arXiv:1801.01112.

Form Factor

$$\langle \eta_c(k)|\bar{c}\gamma_\mu b|B_c(p)\rangle = \left[(p+k)_\mu - \frac{m_{B_c}^2 - m_{\eta_c}^2}{q^2} q_\mu\right] F_1(q^2) + q_\mu \frac{m_{B_c}^2 - m_{\eta_c}^2}{q^2} F_0(q^2)\,,$$

$$\langle J/\psi(k)|\bar{c}\gamma^\mu b|B_c(p)\rangle = -\frac{2iV(q^2)}{m_{B_c}+m_{J/\psi}}\,\varepsilon^{\mu\nu\rho\sigma}\,\epsilon_\nu^*\,p_\rho\,k_\sigma\,,$$

$$\begin{aligned}\langle J/\psi(k)|\bar{c}\gamma^\mu\gamma^5 b|B_c(p)\rangle = {} & 2m_{J/\psi}A_0(q^2)\frac{\epsilon^*\cdot q}{q^2}q^\mu + (m_{B_c}+m_{J/\psi})A_1(q^2)\left[\epsilon^{*\mu} - \frac{\epsilon^*\cdot q}{q^2}q^\mu\right] \\ & - A_2(q^2)\frac{\epsilon^*\cdot q}{m_{B_c}+m_{J/\psi}}\left[p^\mu + k^\mu - \frac{m_{B_c}^2 - m_{J/\psi}^2}{q^2}q^\mu\right]\,,\end{aligned}$$

where the form factors are parametrized as $F(q^2) = F(0)\,\exp(c_1\hat{s} + c_2\hat{s}^2)$ with $\hat{s} = q^2/m_{B_c}^2$ in the full kinematical range of q^2, of which the results computed in the covariant light-front quark model.

Form Factor

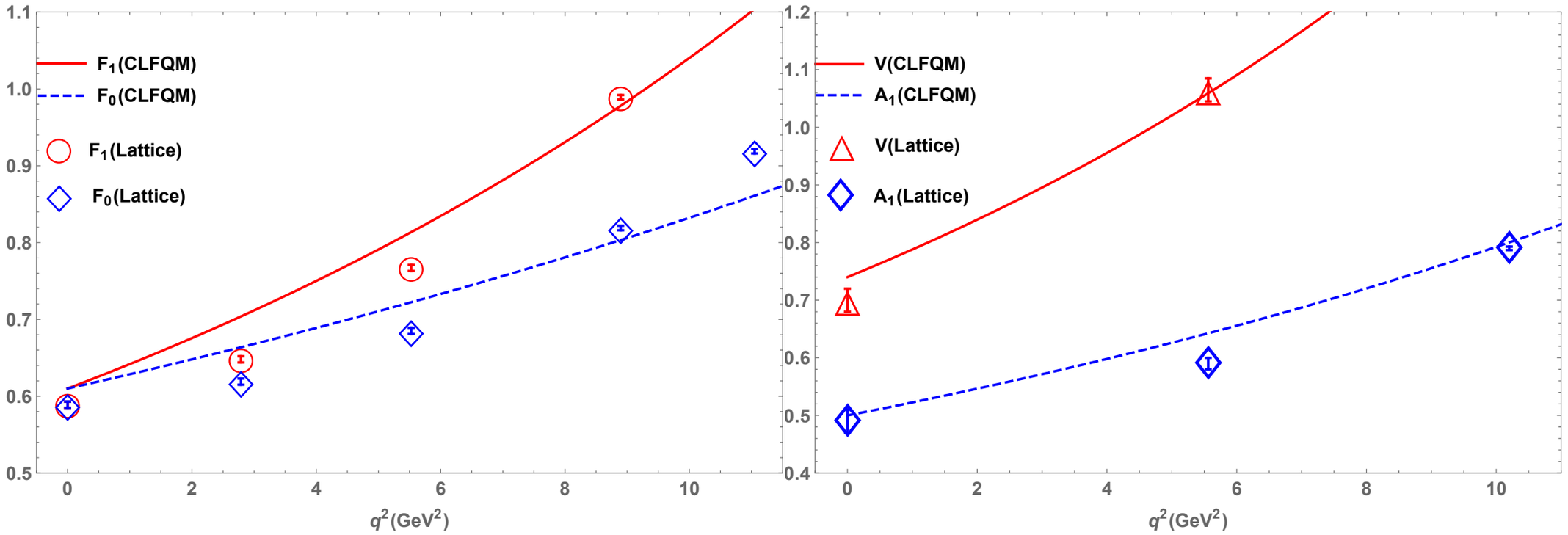


Figure: CLFQM form factors for the $B_c \to \eta_c$ and $B_c \to J/\psi$ hadronic transitions in comparison with the preliminary lattice results.

W. Wang, Y.-L. Shen, and C.-D. Lu, Phys. Rev. D79, 054012 (2009), 0811.3748.

A. Lytle, B. Colquhoun, C. Davies, J. Koponen, and C. McNeile, [arXiv:1605.05645].

B. B. Colquhoun, C. Davies, J. Koponen, A. Lytle, and C. McNeile, [arXiv:1611.01987].

Form Factor

$T(q^2)$ have not been calculated in CLFQM but can be related to $V(q^2)$ and $A(q^2)$ through the quark level equations of motion:

$$F_T(q^2) = -\frac{(m_b + m_c)}{q^2}(m_{B_c} + m_{\eta_c})\big(F_0(q^2) - F_1(q^2)\big)\,,$$

$$T_1(q^2) = \frac{m_b + m_c}{m_{B_c} + m_{J/\psi}} V(q^2)\,,$$

$$T_2(q^2) = \frac{m_b - m_c}{m_{B_c} - m_{J/\psi}} A_1(q^2)\,,$$

$$T_3(q^2) = -\frac{m_b - m_c}{q^2}\Big[m_{B_c}\big(A_1(q^2) - A_2(q^2)\big) + m_{J/\psi}\big(A_2(q^2) + A_1(q^2) - 2A_0(q^2)\big)\Big]\,,$$

where we use the quark masses in the $\overline{MS}$ renormalization scheme at the scale $\mu = \overline{m}_b$ and to be more conservative consider the differences in the numerical results induced by using the pole quark masses as a source of systematic uncertainties.

Method

χ^2 as a function of the Wilson coefficient C_X:

$$\chi^2(C_X) = \sum_{m,n=1}^{\text{data}} (O^{th}(C_X) - O^{exp})_m (V^{exp} + V^{th})^{-1}_{mn} (O^{th}(C_X) - O^{exp})_n + \frac{(R^{th}_{J/\psi}(C_X) - R^{exp}_{J/\psi})^2}{\sigma^2_{R_{J/\psi}}},$$

Table: Experimental data used in the fit.

	R_D	R_{D*}	Correlation	$P_\tau(D^*)$	$R_{J/\psi}$
BABAR, 12	0.440(58)(42)	0.332(24)(18)	−0.27	–	–
Belle, 15	0.375(64)(26)	0.293(38)(15)	−0.49	–	–
Belle, 16	–	0.302(30)(11)	–	–	–
Belle, 17	–	$0.270(35)(^{+0.028}_{-0.025})$	0.33	$-0.38(51)(^{+0.21}_{-0.16})$	–
LHCb, 15	–	0.336(27)(30)	–	–	–
LHCb, 18	–	0.291(19)(26)(13)	–	–	–
LHCb, 18	–	–	–	–	0.71(17)(18)

Numerical Results

Table: Fitted values of the Wilson coefficients in different NP scenarios.

NP scenario	value	χ^2/dof	Correlation
C_{V_1}	$(1+Re[C_{V_1}])^2+(Im[C_{V_1}])^2=1.27(6)$	7.42/8	–
C_{V_2}	$0.057(50)\pm 0.573(73)i$	6.19/8	0.750
C_{S_1}	$0.405(91)$	15.5/8	–
C_{S_2}	$-1.05(30)\pm 1.09(12)i$	5.98/8	0.589
C_T	$0.24(11)\pm 0.13(8)i$	8.39/8	-0.993

1σ Constraints on the NP Scenarios

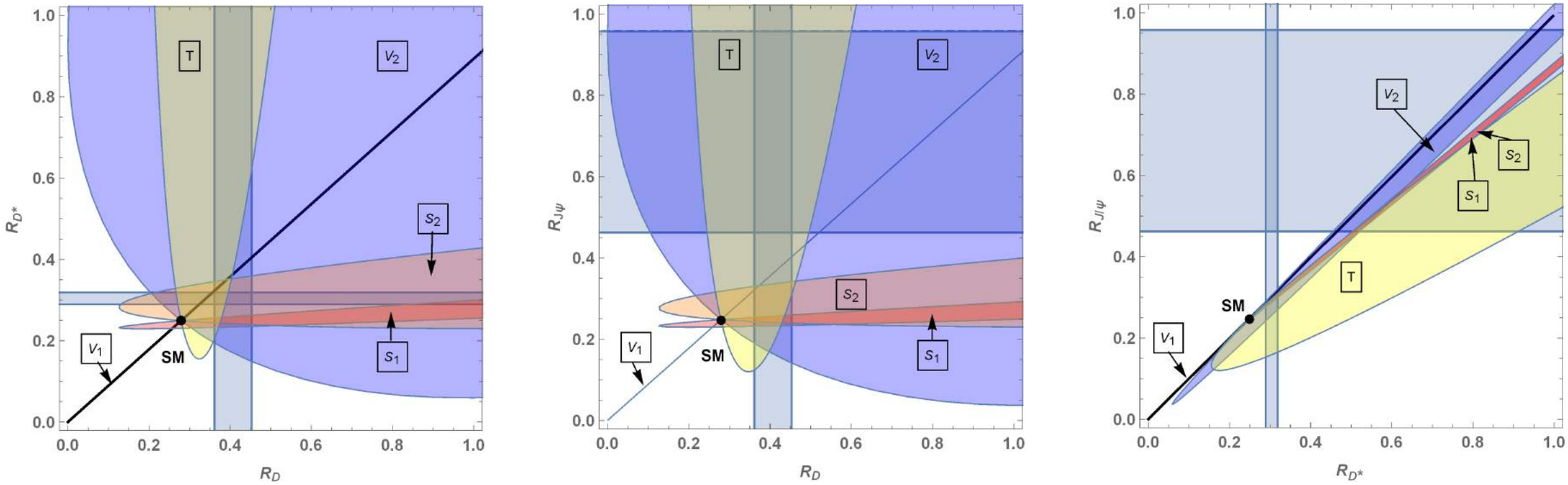


Figure: Correlations between $R(D)$, $R(D^*)$ and $R(J/\psi)$ in the presence of single NP operators. The vertical and horizontal bands show the experimental constraints and the black dots denote the SM predictions.

2σ Constraints on the NP Wilson coefficients

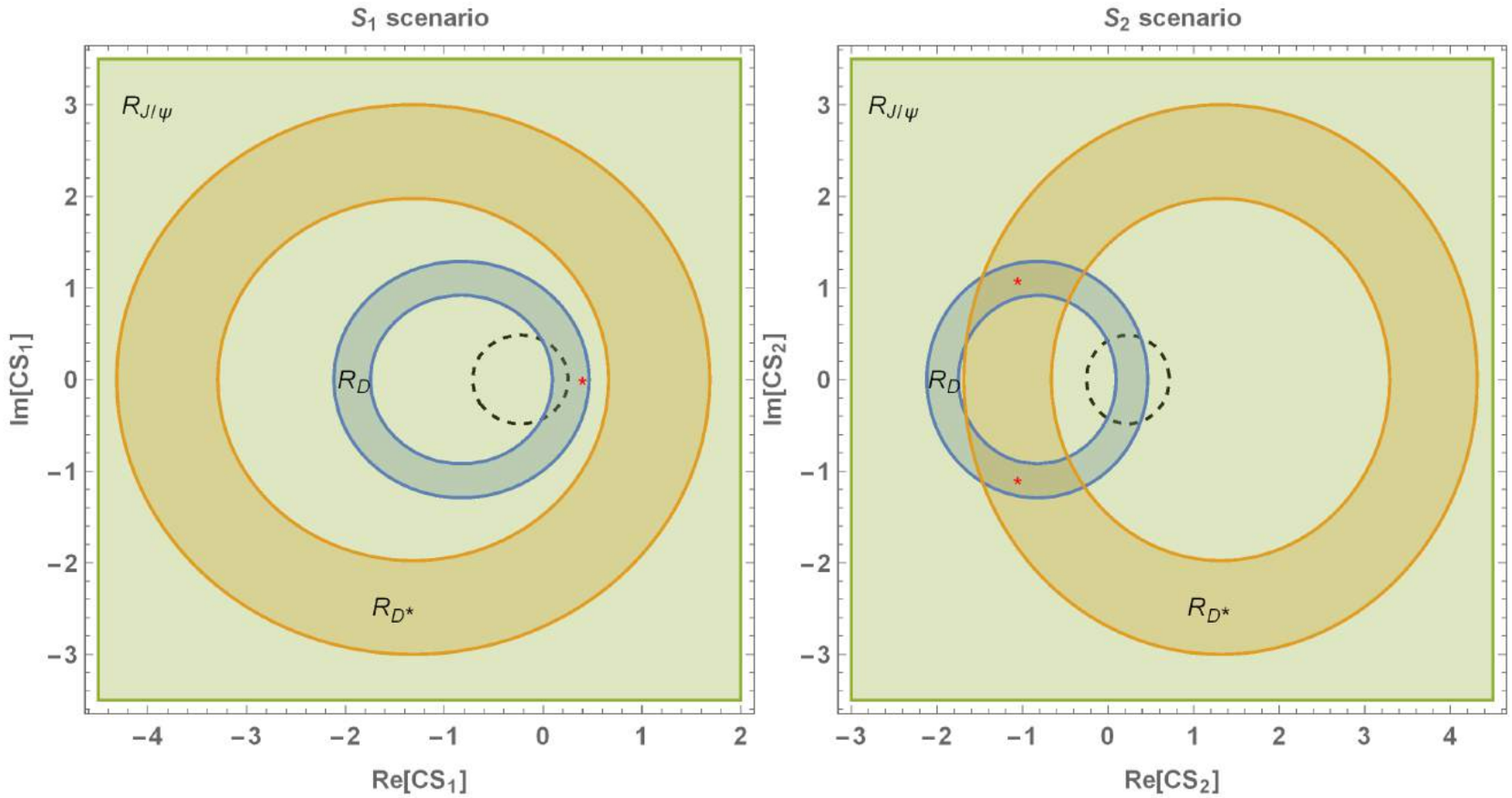
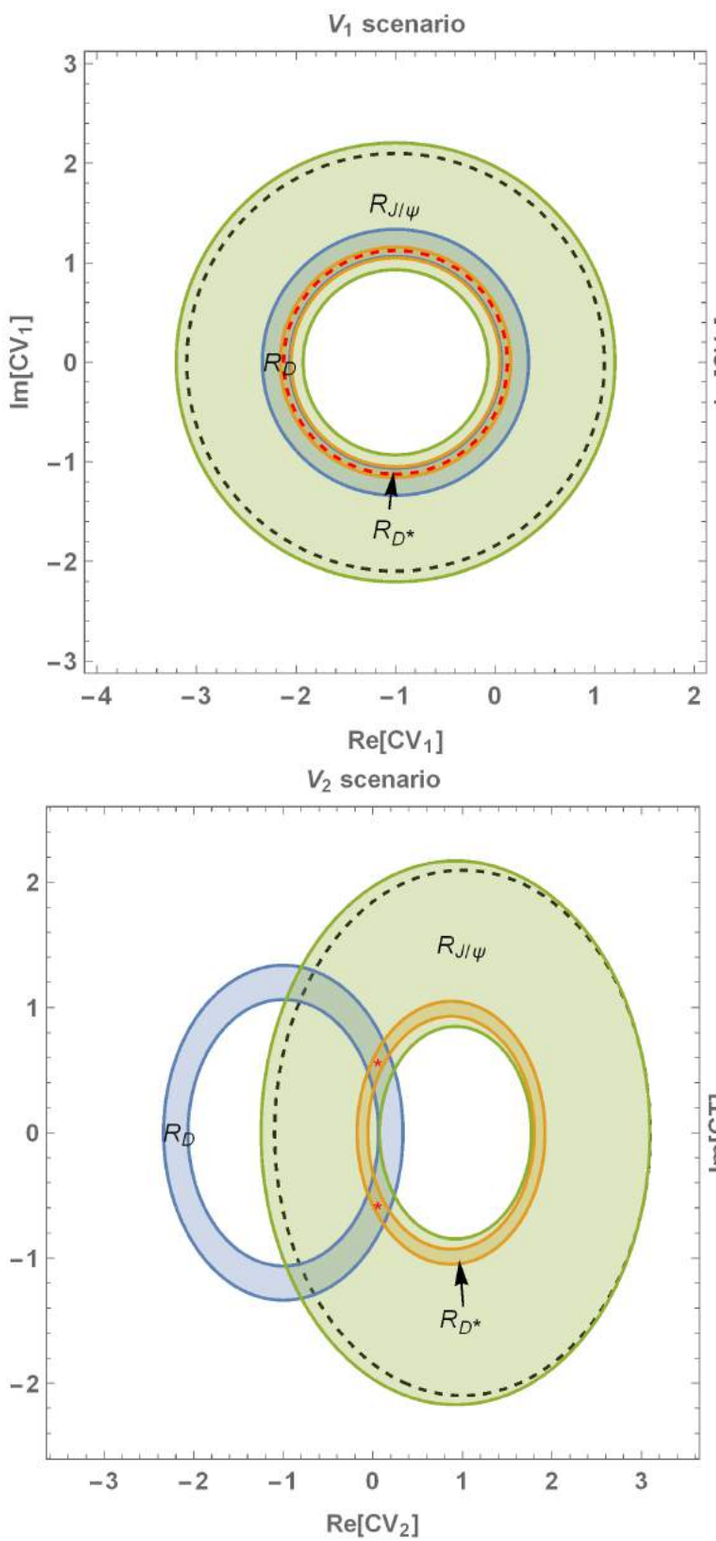
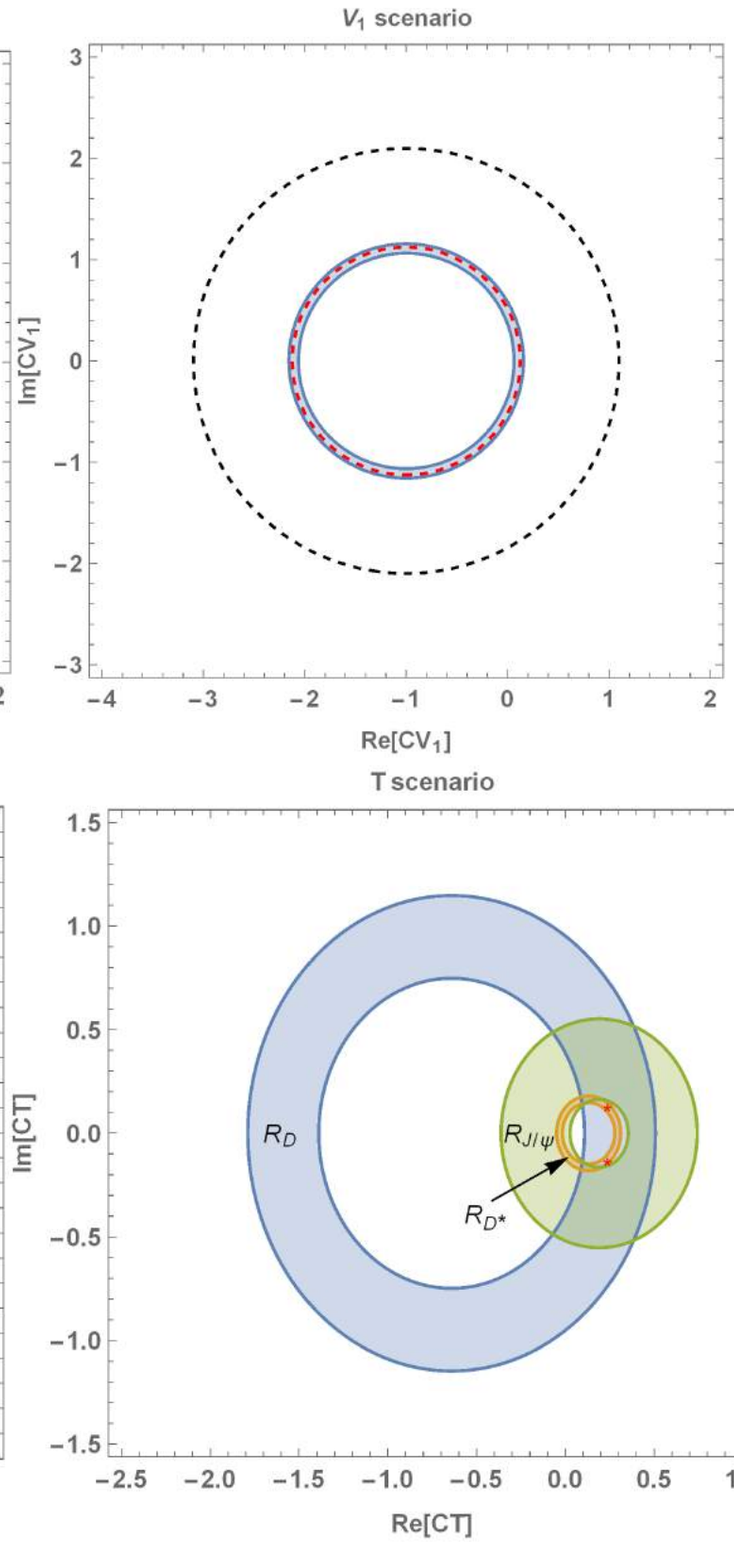




Figure: Constraints on the Wilson coefficients from the measurements of $R(D^{(*)})$ and $R(J/\psi)$ at the C.L. of 2σ and the branching fraction $Br(B_c \to \tau\nu)$ (black dashed curves). In each panel the red stars or dashed curves denote the optimal values obtained by using the fitted Wilson coefficients.

2σ Constraints on the NP Wilson coefficients









Predictions

Table: Predictions for observables involved in the $B \to D^{(*)}$ decays. The first and second uncertainties respectively result from the input parameters and the fitted Wilson coefficients.

Scenario	$R(D)$	$R(D^*)$	$P_\tau(D)$	$P_\tau(D^*)$	P_{D^*}	$\mathcal{A}_{FB}(D)$
SM	0.279(7)(0)	0.249(4)(0)	0.325(3)(0)	−0.508(4)(0)	0.441(6)(0)	0.3606(6)(0)
V_1	0.354(9)(19)	0.317(5)(17)	0.325(3)(0)	−0.508(4)(0)	0.441(6)(0)	0.3606(6)(0)
V_2	0.403(10)(48)	0.307(5)(15)	0.325(3)(0)	−0.509(4)(1)	0.436(7)(4)	0.3606(6)(0)
T	0.371(10)(42)	0.313(26)(15)	0.180(5)(49)	0.038(1)(118)	0.173(11)(60)	0.4311(5)(29)

$$R(D) = 0.407 \pm 0.039 \pm 0.024$$
$$R(D^*) = 0.304 \pm 0.013 \pm 0.007$$

Table: Predicted ranges for observables involved in the $B \to D^{(*)}$ decays from the experimental constraints within 2σ and the limit of $Br(B_c \to \tau\nu)$.

Senario	$R(D)$	$R(D^*)$	$P_\tau(D)$	$P_\tau(D^*)$	P_{D^*}	$\mathcal{A}_{FB}(D)$
V_1	[0.315, 0.373]	[0.282, 0.334]	[0.325, 0.325]	[−0.508, −0.508]	[0.441, 0.441]	[0.361, 0.361]
V_2	[0.315, 0.499]	[0.274, 0.334]	[0.325, 0.325]	[−0.511, −0.508]	[0.429, 0.441]	[0.361, 0.361]
T	[0.321,0.323]	[0.274, 0.334]	[0.248, 0.249]	[−0.234, −0.182]	[0.287, 0.306]	[0.395, 0.398]

Predictions

Table: Predictions for observables involved in the $B_c \to \eta_c(J/\psi)$ decays. The first, second and third uncertainties respectively result from the input parameters, the fitted Wilson coefficients and the quark mass schemes for the tensor form factors.

Scenario	$R(\eta_c)$	$R(J/\psi)$	$P_\tau(J/\psi)$
SM	$0.281(^{+0.034}_{-0.030})(0)$	$0.248(6)(0)$	$-0.512(^{+0.021}_{-0.016})(0)$
V_1	$0.357(^{+0.044}_{-0.038})(19)$	$0.315(7)(17)$	$-0.512(^{+0.021}_{-0.016})(0)$
V_2	$0.406(^{+0.050}_{-0.044})(49)$	$0.304(7)(16)$	$-0.512(^{+0.021}_{-0.016})(1)$
T	$0.337(^{+0.019}_{-0.015})(26)(15)$	$0.188(^{+0.017}_{-0.012})(10)(21)$	$-0.028(^{+0.016}_{-0.013})(175)(53)$

$P_\tau(\eta_c)$	$P_{J/\psi}$	$\mathcal{A}_{FB}(\eta_c)$	$\mathcal{A}_{FB}(J/\psi)$
$0.347(81)(0)$	$0.446(6)(0)$	$0.364(^{+0.007}_{-0.009})(0)$	$-0.042(11)(0)$
$0.347(81)(0)$	$0.446(6)(0)$	$0.364(^{+0.007}_{-0.009})(0)$	$-0.042(11)(0)$
$0.347(81)(0)$	$0.443(6)(3)$	$0.364(^{+0.007}_{-0.009})(0)$	$0.031(7)(13)$
$0.24(^{+0.15}_{-0.13})(4)(2)$	$0.271(14)(64)(41)$	$0.419(^{+0.014}_{-0.031})(23)(8)$	$-0.036(^{+0.010}_{-0.008})(49)(21)$

$$R(J/\psi) = 0.71 \pm 0.17 \pm 0.18 \quad \text{LHCb}$$

PRL120, 121801 (2018)

Predictions

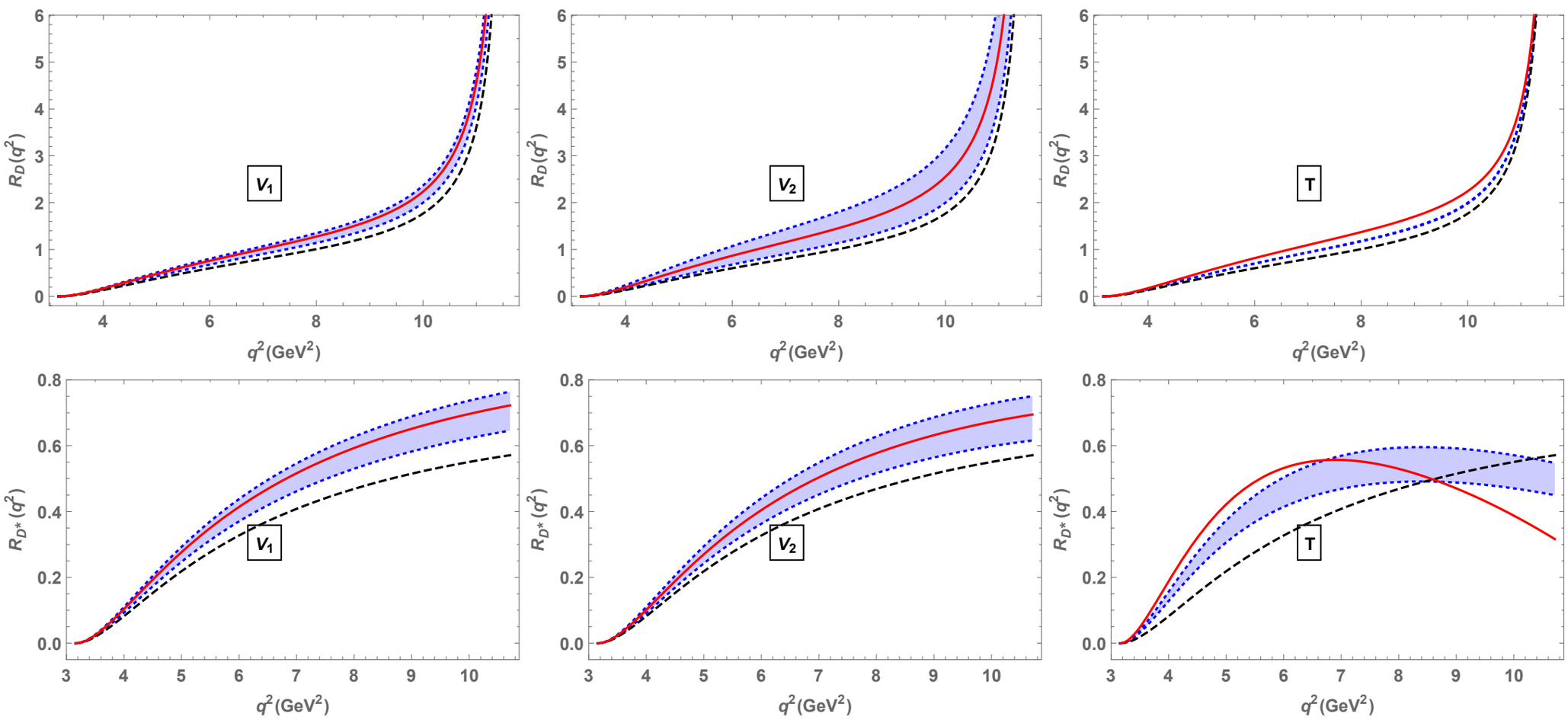


Figure: Predictions for the differential ratios $R_D(q^2)$ and $R_{D^*}(q^2)$. The black dashed lines and the red solid lines respectively denote the SM predictions and the NP predictions corresponding to the best fitted Wilson coefficients. The light blue bands include NP effects corresponding to the experimental constraints within 2σ.

Predictions

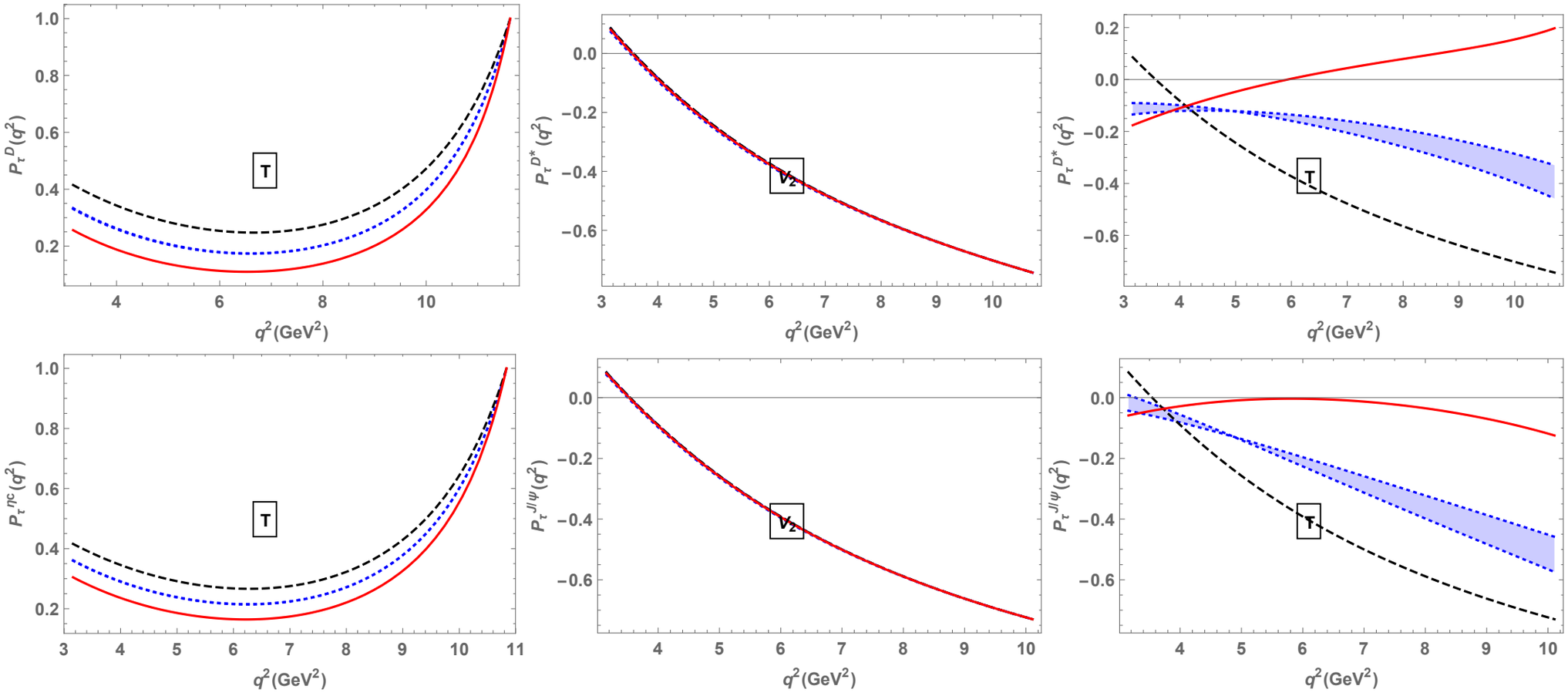


Figure: Predictions for the differential polarizations $P_\tau^{D^{(*)}}(q^2)$, $P_\tau^{\eta_c}(q^2)$ and $P_\tau^{J/\psi}(q^2)$. The black dashed lines and the red solid lines respectively denote the SM predictions and the NP predictions corresponding to the best fitted Wilson coefficients. The light blue bands include NP effects corresponding to the experimental constraints within 2σ.

Predictions

$$P_{\mathcal{M}} = \frac{\Gamma(\lambda_M = 0)}{\Gamma(\lambda_M = 0) + \Gamma(\lambda_M = 1) + \Gamma(\lambda_M = -1)}$$

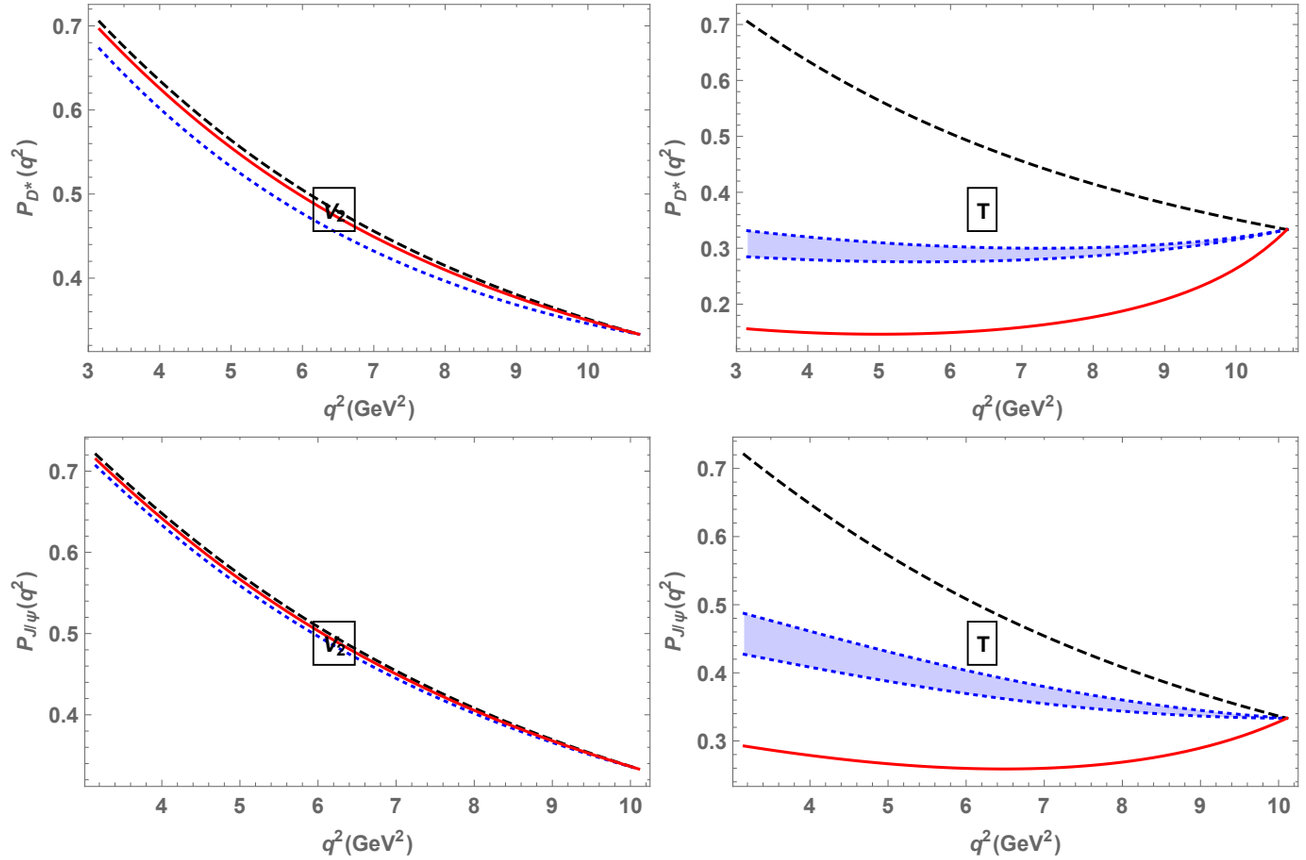


Figure: Predictions for the differential polarizations $P^{D^*}(q^2)$ and $P^{J/\psi}(q^2)$. The black dashed lines and the red solid lines respectively denote the SM predictions and the NP predictions corresponding to the best fitted Wilson coefficients. The light blue bands include NP effects corresponding to the experimental constraints within 2σ.

Predictions

$$\mathcal{A}_{\rm FB} = \frac{\int_0^1 \frac{d\Gamma}{d\cos\theta} d\cos\theta - \int_{-1}^0 \frac{d\Gamma}{d\cos\theta} d\cos\theta}{\int_{-1}^1 \frac{d\Gamma}{d\cos\theta} d\cos\theta},$$

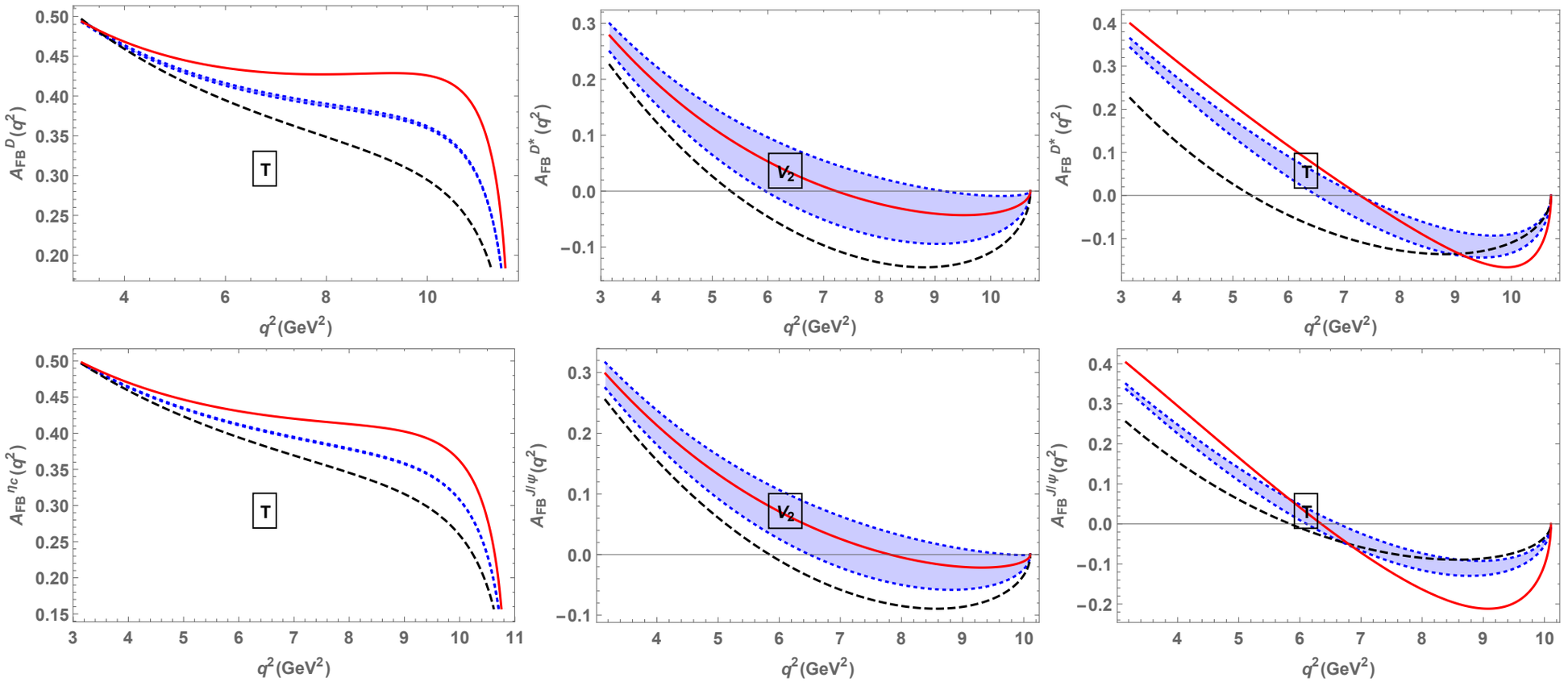


Figure: Predictions for the differential forward-backward asymmetries. The black dashed lines and the red solid lines respectively denote the SM predictions and the NP predictions corresponding to the best fitted Wilson coefficients. The light blue bands include NP effects corresponding to the experimental constraints within 2σ.

Summary

- We have performed a model-independent analysis of the new physics effects in the $b \to c\tau\nu$ transitions within the framework of the effective theory. The improved HQET form factors and CLFQM form factors have been adopted.

- None of the single operators can explain the current experimental measurements of the ratios R(D), R(D$*$) and R(J/ψ) at the confidence level of 1σ simultaneously. Allowed regions for the Wilson coefficients of the vector and tensor operators (severely constrained) are obtained from the experimental constraints within 2σ along with the limit $Br(B_c \to \tau\nu) < 10\%$ from the LEP1 data.

- The predicted R(D) and R(D$*$) using the best fitted Wilson coefficients in the V2 scenario are in excellent agreement with the current world average values.

- Our results suggest that any NP model dominated by a single scalar or tensor operator is under challenge, such as some types of charged Higgs models.

- We have made predictions using the constraints on various physical observables for the $B \to D(*)\tau\nu$ and $B_c \to \eta_c(J/\psi)\tau\nu$ decays, namely R, P_τ , P_M , and A_{FB} , and the corresponding q2 differential distributions.